Research Article

# Enhancement in the tribological properties of Cr/DLC multilayers in methane: structural transformation induced by sliding

Lin Chen[1,2] · Kun Liu[1] · Xubing Wei[1,2] · Zhibin Lu[1,2] · Ning Ren[1,2] · Guangan Zhang[1,2] · Qunji Xue[1,2]

Received: 14 August 2019 / Accepted: 17 October 2019 / Published online: 24 October 2019


**Abstract**
Diamond-like carbon (DLC) films respond as a lubricating material under some atmosphere conditions, such as $N_2$, moisture. Nevertheless, incomplete knowledge about the key factors, which control the performances of film under distinct gases, limits the further use of them. Herein, the tribological properties of DLC film and Cr/DLC multilayers with different modulation periods were studied under methane. Frictional tests conducted under methane show that Cr/DLC film exhibits a great reduction in friction and wear compared to that of DLC film. An interpretation for tribological performances of films was proposed by considering repassivation and structural transformation taking place at the sliding interface. It is chemical passivation that plays a major role in the tribological properties of DLC film, while the Cr/DLC multilayers possess the lower friction coefficient because of the structural transformation induced by shearing. This study is important for broadening applications of DLC film in the industrial field and reducing energy waste.

**Keywords** Cr/DLC multilayers · Passivation · Structural lubrication · Tribological behavior

## 1 Introduction

The presence of friction is necessary for us to walk. Nevertheless, friction in all kinds of moving mechanical components, from automobiles to manufacturing operations, consumes about twenty percent of the annual energy consumption on earth [1], leading to an adverse impact on economy and environment. As such, approaches to control and mitigate friction are significant for the prolongation of mechanical devices lifetime, reduction in energy waste and conservation of environment [2–4]. Heretofore, carbon, as an element, has provided lots of possibilities for production and design of devices, both macro and micro, to exploit in a wide range of applications [5–8]. Coatings containing carbon (both a primary or secondary constituent) were also applied in many fields [9–11]. Particularly, carbon-based films, such as diamond and diamond-like carbon (DLC), exhibit high thermal conductivity, chemical inertness and exceptional mechanical properties.

Currently, DLC films have been examined as a potential material to offer a myriad of tribological, mechanical, biomedical electrical and optical properties [12–14]. Specifically, some films have been considered as potential solid lubricating materials for many engineering fields [15–17]. Thanks to the comprehensive research activities, many methods such as deposition technologies [18, 19], doped elements or a multilayer architecture [20], nanostructures [21, 22] were set up to improve the tribological properties of film. However, DLC films were extremely sensitive

**Electronic supplementary material** The online version of this article (https://doi.org/10.1007/s42452-019-1521-1) contains supplementary material, which is available to authorized users.

✉ Zhibin Lu, zblu@licp.cas.cn; ✉ Guangan Zhang, gazhang@licp.cas.cn | [1]State Key Laboratory of Solid Lubrication, Lanzhou Institute of Chemical Physics, Chinese Academy of Sciences, Lanzhou 730000, China. [2]Center of Materials Science and Optoelectronics Engineering, University of Chinese Academy of Sciences, Beijing 100049, China.

to the synthesis and environmental conditions [23–25]. Therefore, exploring the key parameters that cause the low friction of films during relative sliding is quite necessary. In general, surface dangling bonds across the sliding interface of DLC film could be produced by shearing, leading to a high friction. So, a fast surface repassivation is a precondition for low friction of DLC film. The prevailing views about repassivation mechanisms are chemical termination and rehybridization. Chemical termination has been proved by experiments and simulations [26–28]. For example, DLC film exhibited lower wear and friction under humid environments than under vacuum or dry gas [29]. Large-scale density-functional tight-bonding (DFTB) molecular dynamics (MD) simulations pointed out that groups dissociated from water passivated the dangling bonds across the sliding interface, thus leading to low friction [28]. For rehybridization, it was controversial that graphitization at the sliding interface resulted in low friction. In addition, graphitization was considered as the result of shear-induced amorphization [30, 31]. The other promising and interesting methods proposed for achieving ultra-low friction are structural superlubricity. The theoretical reason of structural superlubricity is that inherent geometry of sliding interface causes the weak interaction and vanishing friction occurs [32]. Designing multilayer architecture to reduce friction coefficient and wear rate was due to the improvement of toughness and hardness. Multilayer architecture that a good combination of chromium and DLC layer thickness resulted in a best high hardness, fracture toughness and tribological behavior of film [33]. Nevertheless, further consideration and explanation are required for the peculiarities or intriguing points of these films under various conditions. For instance, green energy such as hydrocarbons has become a focus of each country with the development of economy, yet there are lacks in the studies of the mechanism for DLC films under hydrocarbon gases, which limits their application in other industrial fields, such as natural gas vehicle, seal valve of a gas pipeline and engines [34].

Herein, considering the tribological and mechanical properties of DLC film could be improved by design with multilayer, the tribological properties of DLC film and Cr/DLC multilayers under methane were explored. The tests that a-C film and Cr/DLC films with different modulation periods slid against 9Cr18 balls were carried out under methane. It was observed that chemical passivation of dangling bonds across the sliding interface was essential for the low friction and wear of DLC film. Meanwhile, the existence of Cr layer had significant influence in the structure of DLC layer, leading to the distinct tribological properties of film. In addition, low friction coefficient of Cr/DLC film was attributed to the structure where Cr grains were inlaid in DLC material. Therefore, tribological performances of Cr/DLC film in methane were discussed, which broadened its applications in industrial field and reduced energy waste.

## 2 Experimental section

### 2.1 Film deposition

Multilayers of Cr/DLC were prepared on (100) silicon wafers and 3 cm × 3 cm × 0.3 cm square shape 304C stainless steel (SS) sheets by a multi-target magnetron sputtering system with a pulsed-DCMS process. The substrates were ultrasonically degreased in mineral ether, acetone and alcohol for 15 min prior to film deposition. Then the substrates were sputtered with argon ions for 15 min to remove the surface oxide. After that, surface activation was achieved, too. A Cr interlayer (~ 300 nm) was deposited between multilayers and substrate to enhance their adhesion strength [35]. Three targets (two Cr targets and one graphite target) were placed side by side to prevent cross-contamination of the target material. Meanwhile, the graphite target was placed in the middle. Then the rotation of the specimen holder resulted in the uniform multilayer structure of films. Therefore, uniform Cr/DLC multilayers with different modulation periods were obtained by controlling deposition time of DLC layers. The specific deposition parameters in this study are summarized in Table 1. Besides, the presupposed structures of films are shown in Table 2. Here, one Cr layer and one DLC layer in multilayers are called one modulation period.

**Table 1** Cr/DLC deposition conditions

| | Chamber pressure (Pa) | Substrate pulsed bias (V) | Target current (A) | Average target power density ($10^4$w/m$^2$) | Time (min) |
|---|---|---|---|---|---|
| Clean with Ar sputtering | 0.8 | − 500 | – | – | 15 |
| Interlayer | | − 300 | 2.0 (Cr) | 6.9 | 15 |
| Cr/DLC deposition | | − 70 | 1.0 (Cr) | 3.5 | 0.5 (Cr) |
| | | − 70 | 1.2 (C) | 5.9 | 2–6 (C) |

**Table 2** Modulation period, number of interfaces and total thickness of Cr/DLC multilayers

| Sample no. | D1 | D2 | D3 | D4 | D5 | D6 |
|---|---|---|---|---|---|---|
| Modulation period/nm | – | 82.5 ± 1.2 | 70.8 ± 0.8 | 58.9 ± 2.1 | 47.2 ± 0.7 | 31.4 ± 3.7 |
| Number of interfaces | – | 76 | 86 | 100 | 120 | 150 |
| Total thickness/μm | 1.47 ± 0.04 | 3.19 ± 0.13 | 3.10 ± 0.14 | 3.03 ± 0.18 | 3.00 ± 0.14 | 2.65 ± 0.07 |

### 2.2 Film characterization

Surface morphology of films was measured by a CSPM 4000 atomic force microscopy with a scanning frequency of 5 Hz. Fractured cross-sectional investigation of films was conducted by SU8020 field emission scanning electron microscope. The transmission electron microscopy (TEM) sample was prepared by focused ion beam (FIB) technology. Then the investigation of microstructure of multilayers was carried on a FEI Tecnai G2 F20 TEM instrument. X-ray diffraction (XRD) on a Philip X' pert diffractometer with a glancing angle of 1° was utilized for crystallographic investigation of these films. Then elastic modulus and hardness were obtained by Anton Paar TTX-NHT3 Nanoindenter with a depth limit of 100 nm. Vickers indentation method was used to determine film toughness, and the effective fracture toughness ($K_C$) can be expressed as a function of radial crack size ($c$):

$$K_c = \alpha\left(\frac{E}{H}\right)^{1/2}\left(\frac{P}{c^{3/2}}\right) \quad (1)$$

where $\alpha$ is a constant depending on the indentation shape (Berkovich indenters: 0.016); $H$ and $E$ are hardness and elastic modulus of film, respectively; and $P$ is the normal load. Raman spectroscopy was measured by a JY-HR800 Raman spectrometer with an excitation wavelength of 532 nm.

### 2.3 Tribological tests and characterization

The friction tests of samples were carried out by a vacuum tribo-meter fitted with a friction force sensor with an accuracy of 3 mN. The 9Cr18 stainless steel (SS) bearing ball of 6 mm in diameter with a roughness (Sa) of ~ 30 nm was used as the counterpart ball. Meanwhile, all those tests were done under a methane pressure of 250 Pa with a sliding frequency of 2 Hz, an amplitude of 5 mm as well as a normal load of 0.5 N. Besides, the test was repeated three times. After tests, the wear tracks and wear scars were analyzed by a non-contact three-dimensional surface profiler (MicroXAM-800, KLA-Tencor, USA) while the structure was analyzed by a LabRam HR800 Jobin–Yvon spectrometer.

## 3 Results and discussion

### 3.1 Structural and mechanical properties analysis for film

The grown films are relatively smooth without any large particles on the surface in spite of the different modulation period (Fig. S1). It results from basically identical sputtering energy. Thickness and modulation period of film can be obtained by cross-sectional SEM intuitively. Figure 1 shows SEM micrographs of fractured cross sections for films. It indicates all films possess compact structure. Simultaneously, fineness of columnar structure increases gradually, indicating the rising film compactness, with the decreasing modulated period. This is because the loose columnar structure interface in the multilayer film is interrupted. Figure S2 illustrates XRD analysis of crystal structure for Cr in film. All of the Cr layers exhibit the preferential orientation of the (110) plane accompanied by low intensity (200) or (211) reflection. This is consistent with the bcc-Cr structure announced by Arias [36]. Meanwhile, interplanar distance of Cr layer in D3 and D4 films is larger and crystal grain is smaller among these films. It is induced by internal stress and interactions between structures of DLC and Cr layer.

In order to get more detailed structural information, TEM cross-sectional analysis of the Cr/DLC multilayers with a interfaces number of 76 is carried out, as presented in Fig. 2. The Cr interlayer followed by a distinct multilayer structure composed of alternating Cr and DLC layers is shown in Fig. 2a. As shown in Fig. 2b, typical columnar structure with clear columnar boundaries, which is due to interface waves accumulated in the graded region [37], is found in the deposited Cr/DLC multilayers. Figure 2c indicates Cr interlayer is uniform and highly crystalline. However, some mixed region with Cr and DLC structure could be observed from Fig. 2d. The hardness and elastic modulus for films reach maximum and then decrease as the number of interface increases (Fig. 3a). It should be attributed to the finite dislocation movement between and within layers [38, 39]. The high $H/E$ and $H^3/E^2$ ratios indicate high resistance to plastic deformation. Figure 3b shows the $H/E$ and $H^3/E^2$ ratios of the Cr/DLC film increase to a maximum value (D5 film) and then decrease as the increase of the number of interfaces. Moreover, multilayer structure design can enhance toughness [40] and

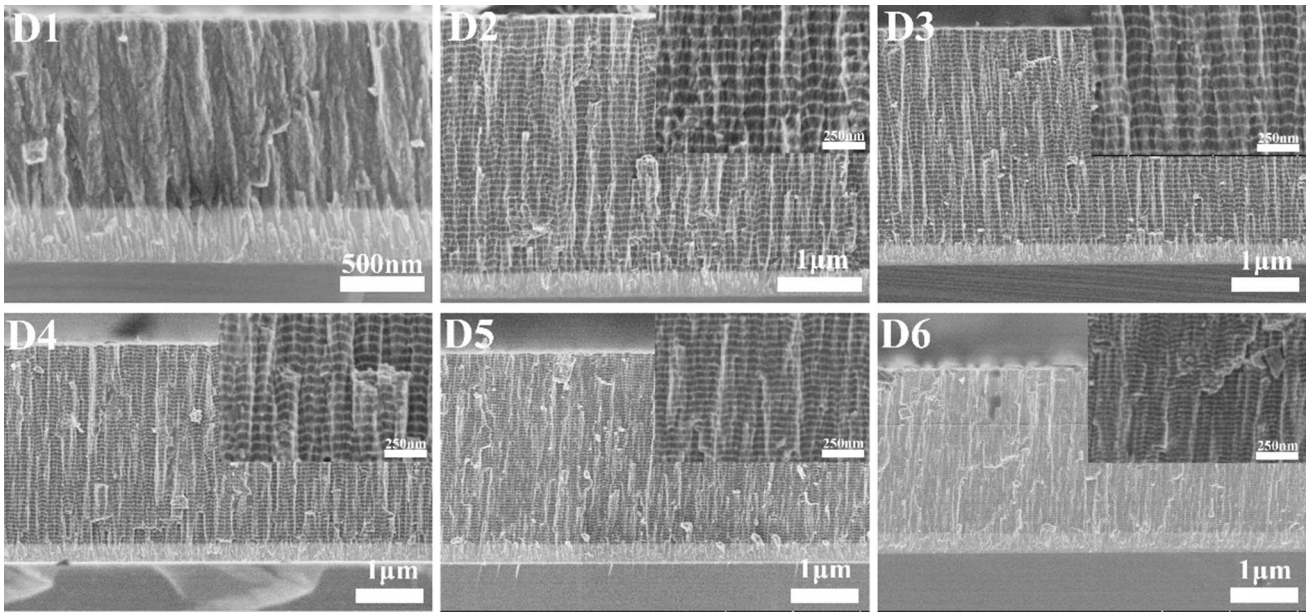


**Fig. 1** SEM micrographs of fractured cross sections for films

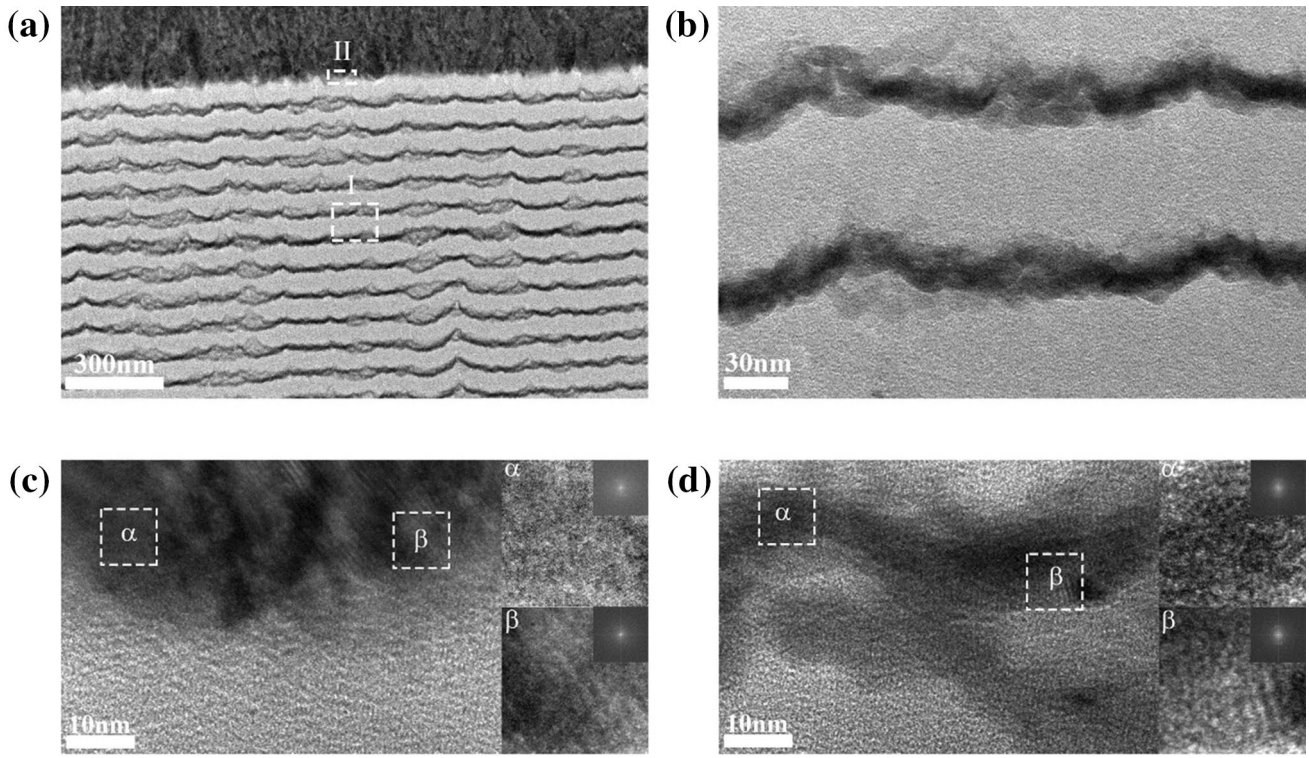


**Fig. 2** TEM cross-sectional images of D2 (**a**). **b**, **c** are enlarged images of I and II in (**a**), respectively. And **d** is information of Cr layer

D5 film exhibits a strong toughness (Fig. S3), determined by the coordination of individual layer thickness and heterogeneous interface number [37]. In fact, toughness of multilayer film is improved because of the increased energy dissipation of crack in the interface and the better ductility. Therefore, D5 film which possesses appropriate thickness ratio exhibits the best toughness and hardness.

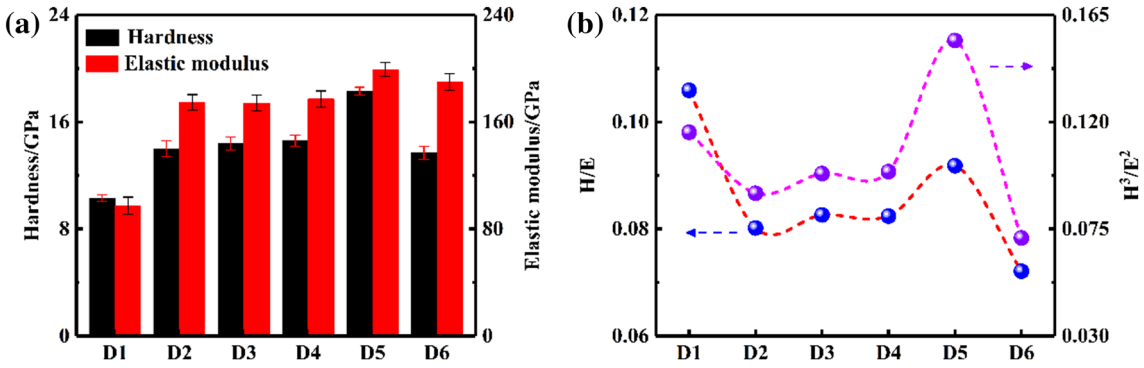


**Fig. 3** Hardness and elastic modulus for DLC and Cr/DLC films (**a**) and the corresponding $H/E$ and $H^3/E^2$ (**b**)

### 3.2 Tribological performances of films

Figure 4 shows friction behaviors of DLC and various Cr/DLC films against the 9Cr18 stainless steel balls under methane. Every film exhibits low friction coefficient after rapidly rising to a high value (Fig. 4a). Moreover, D3 film shows the lowest friction coefficient among all films (Fig. 4b). A longer time test was carried out to elucidate the mechanism of low friction for films (Fig. 4c). It indicates unusual performance for Cr/DLC film compared to DLC film. For DLC film (D1 film), the friction coefficient remains basically constant with small fluctuations. However, the

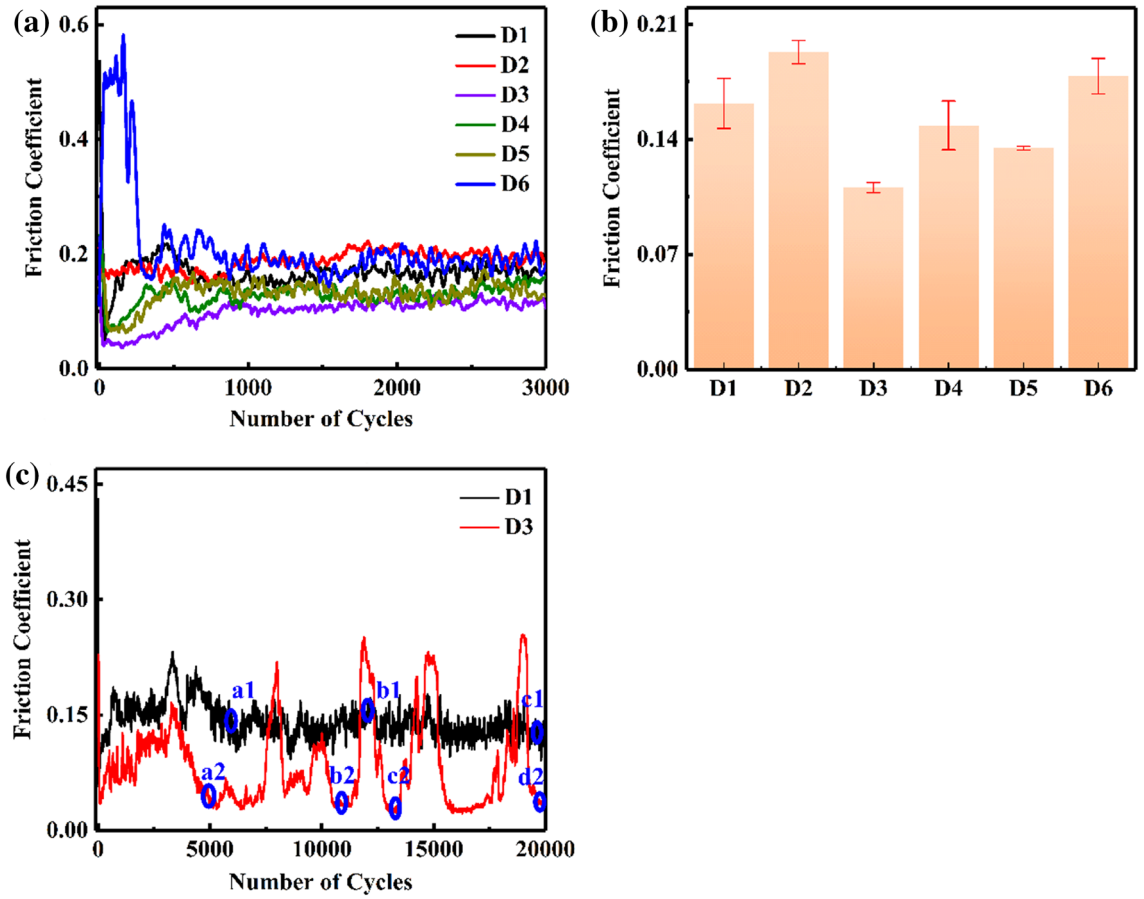


**Fig. 4** Friction behavior of DLC and various Cr/DLC films against the 9Cr18 stainless steel balls under methane (**a**), the corresponding average steady-state friction coefficient (**b**), as well as friction coefficient curves of DLC (D1) and Cr/DLC (D3) films under methane (**c**)

friction coefficient of Cr/DLC film appears wide fluctuations mainly due to the various sliding interface composed of Cr and DLC.

### 3.3 Analysis of wear tracks and wear scars

Figure S4 demonstrates 3D profiles for the wear tracks of films, showing there are many furrows inside the wear tracks and a lot of debris outside the wear tracks. And the corresponding cross-sectional images for the wear tracks are shown in Figs. S5 and S6. It is amazing to find that only one modulation period of D3 film is worn while several modulation periods of others are worn after 3000 sliding cycles. The wear rate of films after 3000 sliding cycles and after various sliding cycles is shown in Fig. 5a, b, separately. It illustrates the wear rate of D3 film is lowest while that of D6 film is highest among all films (Fig. 5a). Moreover, wear of the film could be drastically reduced with the interface formed by multi-layer structure under sliding (Fig. 5b). Besides, according to the friction coefficient (Fig. 4) and cross-sectional images of films (Figs. S5, S6), it is obvious that the friction performance of Cr/DLC films is governed by many factors, such as film structure, passivation, rehybridization.

In order to further reveal the mechanism for low friction of Cr/DLC film, some characterizations such as Raman spectra, nanoindentation as well as TEM were carried out. Figure 6 demonstrates ID/IG of pristine films as well as wear tracks after 3000 sliding cycles. In addition, the corresponding Raman spectra are shown in Fig. S7. The existence of Cr layer increases the content of $sp^3$ C because of the increased compressive stress [38]. It should be noted that ID/IG falls as the number of rings per cluster falls and the fraction of chain groups rises [41]. The difference between ID/IG of DLC and Cr/DLC films indicates that the number of rings per cluster in Cr/DLC film increases.

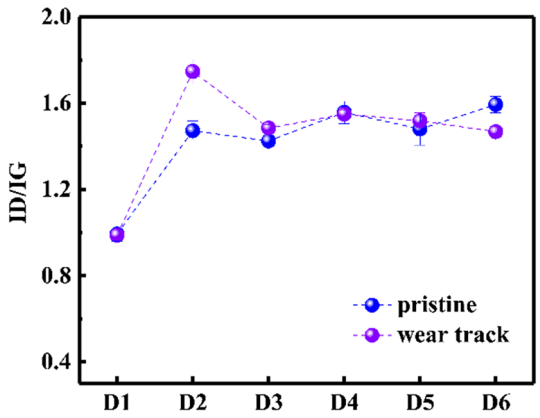


**Fig. 6** ID/IG ratio in function of the pristine films and wear tracks of films after 3000 sliding cycles

Therefore, ID/IG raises although the $sp^3$ C increases. Comparing the results of pristine films, it is found that there is little change in ID/IG of wear scars except that of D2 and D6 tribological systems (Fig. 7). Raman spectra recorded for wear scars of above tests illustrate there is transfer film containing hybridized carbon on the counterpart ball (Fig. S7). Combining Raman spectra with nanoindentation measurement can determine changes in $sp^3$ C content of film [42, 43]. Therefore, nanoindentation tests on wear track of D1 and D3 films with a load of 0.3 mN are used to explore the tribological mechanism. The results are exhibited in Fig. 8. It shows that the hardness in the wear track regions of D1 film increases first and after that it is almost constant with the sliding cycles. ID/IG of wear tracks shows the same trend. Meanwhile, ID/IG reflects that graphitization occurs appreciably in D1 film after 6000 sliding cycles. Thus, it illustrates some of C dangling bonds are passivated with groups dissociated from methane and others bond together in rings at first [44] result in higher

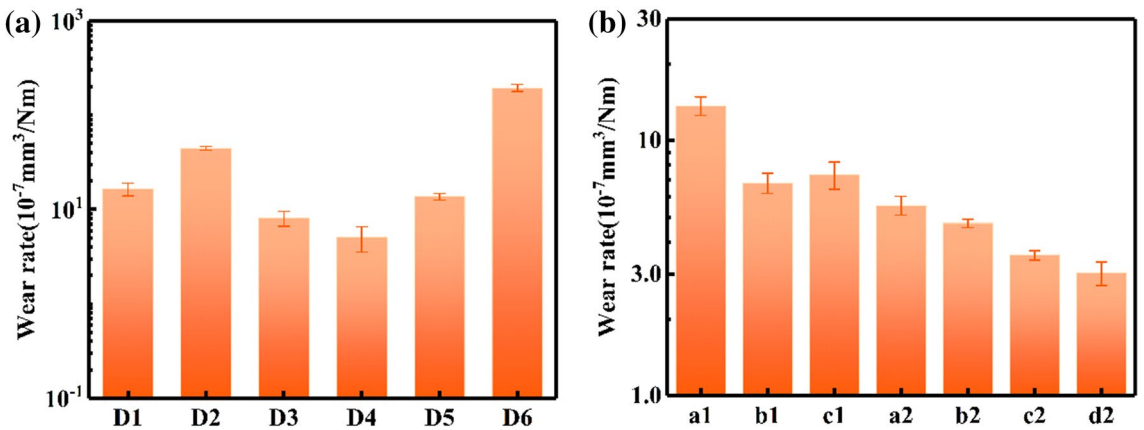


**Fig. 5** Wear rate of films after 3000 sliding cycles (**a**), as well as D1 and D3 films after various sliding cycles (**b**)

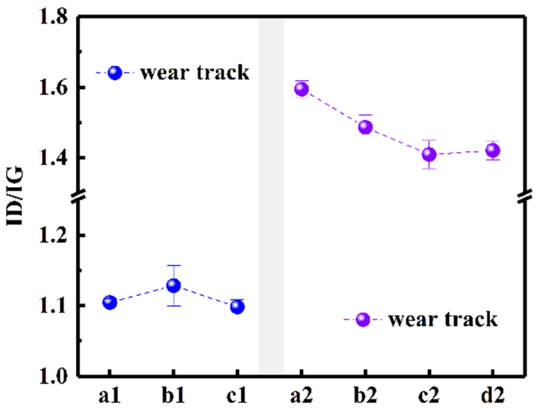


**Fig. 7** ID/IG ratio for wear tracks of D1 and D3 films after various sliding cycles

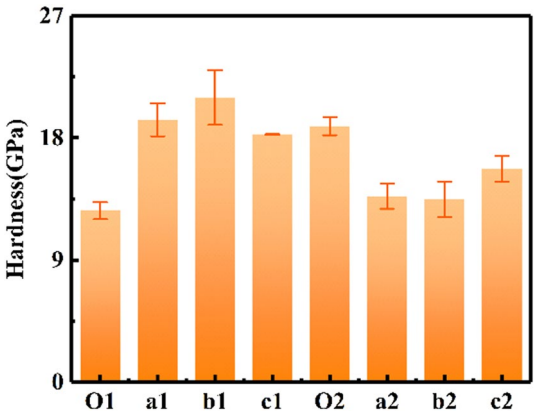


**Fig. 8** Comparison of hardness in the wear track regions of D1 and D3 after various sliding cycles. O1 represents wear track regions of D1 film after 3000 sliding cycles while O2 represents that of D3

hardness. Then more C dangling bonds bond together in rings. However, little change in friction coefficient of films is observed. Therefore, the friction behavior of the film is largely determined by passivation and graphitization has little effect. For D3 film, the hardness in the wear track regions is found to increase first, then decrease and increase again with the increase in sliding cycles. ID/IG for wear track of D3 film increases firstly and then decreases during long time sliding. Therefore, C dangling bonds in D3 are passivated with groups dissociated from methane and others bond together in rings, leading to the increment of hardness and ID/IG. Then Cr is located on the sliding interface, resulting in the low friction (friction coefficient is about 0.03) as well as the change in ID/IG and hardness. Here, the influence of passivation on tribological behavior of film reduces.

To find out the effects of Cr on friction performance of film, transfer films, which is a friction product adhered to the surface on ball during sliding, are collected for TEM analysis. Transfer film on the wear scar was placed on a copper mesh, and transfer film in the middle of sample was observed with TEM. Figure 9 shows transfer film of D1 film is always amorphous during sliding. Grains are observed in transfer film of D3 film in the late sliding cycles. In addition, they are inlaid in amorphous carbon. This structure greatly reduces the friction coefficient. As discussed above, structural lubrication determines the low friction of the Cr/DLC film. Then the schematic description is shown in Fig. 10. The top DLC layer plays an important role in tribological behavior of Cr/DLC film before the appearance of the Cr layer. In particular, the DLC layer transfers to the counterpart ball because of adhesion in sliding interface. Simultaneously, dangling bonds in the sliding interface are passivated by groups from dissociation of methane, resulting in low friction of sliding interface. With further wear, small Cr debris appear at the sliding interface (as shown in part *a* in Fig. 10). The debris of DLC and Cr debris are mixed during the friction process (as shown in part *b* in Fig. 10). At last, structure, in which Cr grains are inlaid in amorphous carbon, is formed by mixed debris with the effect of shear stress. Cr grains enhance the ductility of sliding interface, and a dislocation in the layer requires a high energy because of the existence of interlayer boundary is formed. Consequently, the sliding interface with the above structure is easy to shear between tribological interfaces, resulting in lower friction for sliding system [45].

In summary, the effect of Cr layer on tribology behaviors of DLC film under methane was explored by Cr/DLC film with different modulation periods. Passivation of carbon dangling bonds and structural transformation in sliding interface play a role in tribology properties of films. When Cr layer is introduced, carbon dangling bonds in DLC layer are combined in form of $sp^2$ and $sp^3$, leading to difference in tribological properties between D1 and D3 films (Fig. 4). Besides, interlayer distance of Cr layer has an effect on the tribological behaviors, too. The interlayer distance is too small to move dislocations within itself, so the dislocations between layers require relatively small energy barrier to move. Therefore, D2 film exhibits high friction coefficient and high wear rate. In addition, DLC layer in D6 film is too thin to form a transfer film, resulting in high wear rate. D5 film exhibits low friction coefficient and wear rate due to a suitable DLC layer and low energy barrier to move between layers. D4 film shows a high friction coefficient and wear rate because of the dislocations between and within layers. It must be stated that the structure, in which Cr grains are inlaid in amorphous carbon, occurs in a long sliding process, leading to low friction to a great extent. Nevertheless, destruction of the

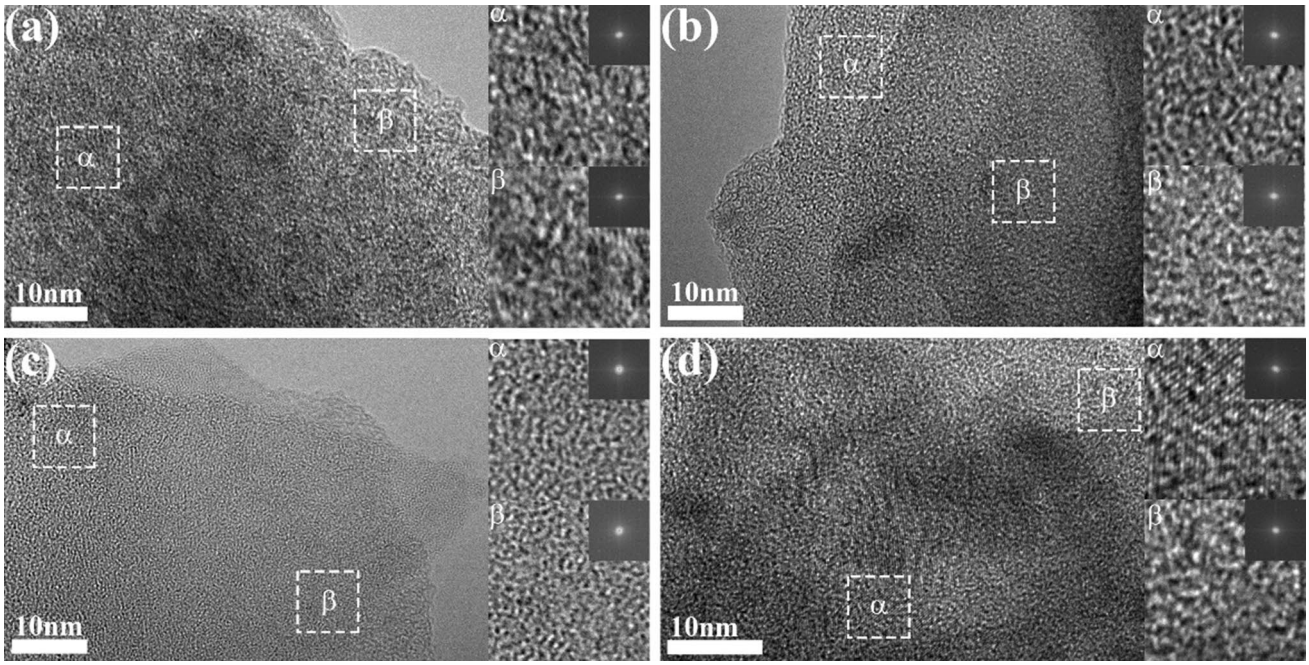


**Fig. 9** TEM images of debris on counterpart balls. Samples in **a** and **b** come from wear scar of D1 after 3000 and 12,000 sliding cycles, separately. Samples in **c** and **d** come from wear scar of D3 after 3000 and 10,500 sliding cycles, separately

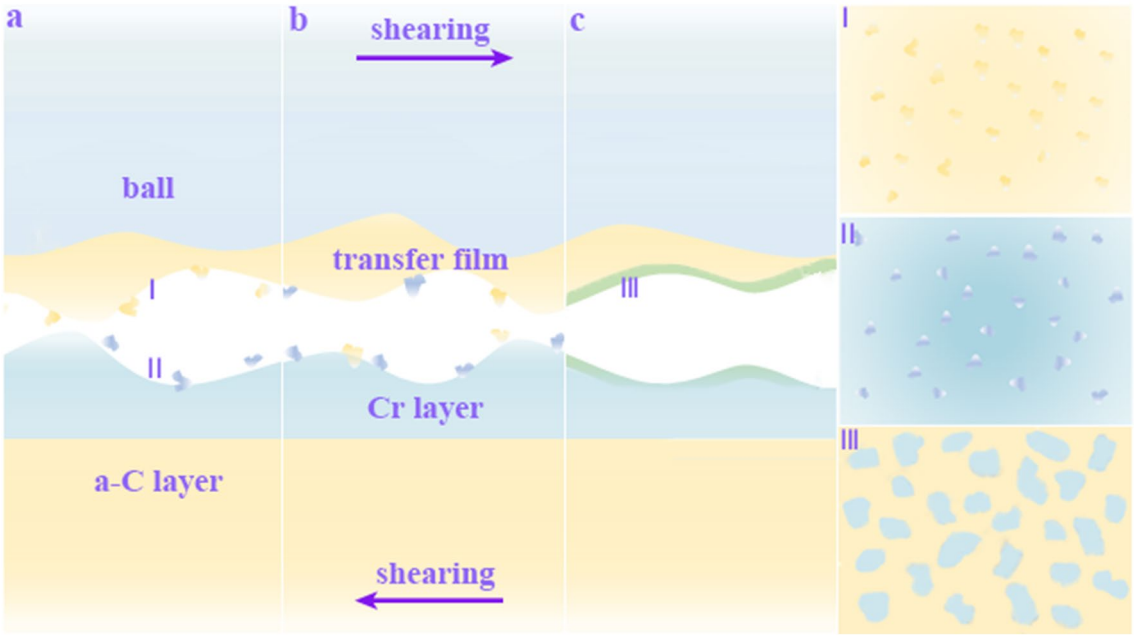


**Fig. 10** Schematic description for formation of lubricating transfer films on Cr/DLC film in the presence of methane molecules. Interfaces I, II and III are marked in part a and c, separately

structure can lead to high friction. Therefore, new design possibilities which are provided with elemental additions and a new structure of DLC layer could further optimize the mechanical properties of DLC layer to obtain a more stable structure with a lower friction coefficient under methane.

## 4 Conclusion

The tests that DLC and Cr/DLC films rubbed with 9Cr18 SS balls are carried to explore the tribological performances of films under methane. According to Raman spectra analysis on carbon bonds in films and TEM on the structure of transfer films, the tribology behaviors of DLC film depend on carbon dangling bonds which are passivated with groups dissociated from methane. For Cr/DLC films, modulation period has a crucial role in the structure and friction performances. The Cr/DLC film with an appropriate modulation period could exhibit low friction and low wear. It is the structure composed of Cr and DLC nanostructure that lows drastically friction of sliding interface. However, further studies on the stability of the structure are indispensable for Cr/DLC film to apply in methane.

**Funding** This work was supported by National Key R&D Program of China (2018YFB0703801); National Natural Science Foundation of China (51775535), Key Projects of Guangxi province science and technology plan (AA18242002).

### Compliance with ethical standards

**Conflict of interest** On behalf of all authors, the corresponding author states that there is no conflict of interest.

## References

1. Holmberg K, Erdemir A (2017) Influence of tribology on global energy consumption, costs and emissions. Friction 5(3):263–284. https://doi.org/10.1007/s40544-017-0183-5
2. Erdemir A, Ramirez G, Eryilmaz OL, Narayanan B, Liao Y, Kamath G, Sankaranarayanan SK (2016) Carbon-based tribofilms from lubricating oils. Nature 536(7614):67–71. https://doi.org/10.1038/nature18948
3. Berman D, Erdemir A, Sumant AV (2013) Reduced wear and friction enabled by graphene layers on sliding steel surfaces in dry nitrogen. Carbon 59:167–175. https://doi.org/10.1016/j.carbon.2013.03.006
4. Berman D, Erdemir A, Sumant AV (2013) Few layer graphene to reduce wear and friction on sliding steel surfaces. Carbon 54:454–459. https://doi.org/10.1016/j.carbon.2012.11.061
5. Cheng Z, Zhang G, Zhang B, Ma F, Lu Z (2018) Tuning the electronic structure of hexagonal boron nitride by carbon atom modification: a feasible strategy to reduce sliding friction. Mater Res Express 6(3):036306. https://doi.org/10.1088/2053-1591/aaf705
6. Zhang B, Zhang G, Cheng Z, Ma F, Lu Z (2019) Atomic-scale friction adjustment enabled by doping-induced modification in graphene nanosheet. Appl Surf Sci 483:742–749. https://doi.org/10.1016/j.apsusc.2019.03.267
7. Palai PK, Mondal A, Chakraborti CK, Banerjee I, Pal K (2019) Green synthesized amino-PEGylated silver decorated graphene nanoplatform as a tumor-targeted controlled drug delivery system. SN Appl Sci. https://doi.org/10.1007/s42452-019-0287-9
8. Liu K, Chen L, Zhang G, Wu G, Ma F, Lu Z (2019) Carbon content and layers number controlling electronic properties of hybridized graphene and boron nitride. Ceram Int. https://doi.org/10.1016/j.ceramint.2019.06.190
9. Bhong SY, More N, Choppadandi M, Kapusetti G (2018) Review on carbon nanomaterials as typical candidates for orthopaedic coatings. SN Appl Sci. https://doi.org/10.1007/s42452-018-0082-z
10. Cao X, Shang L, Liang Y, Zhang G, Lu Z, Xue Q (2019) The tribological performances of the boron carbide films tested under wet air and wet $N_2$ conditions. Tribol Lett. https://doi.org/10.1007/s11249-019-1184-5
11. Lima RMAP, de Oliveira MCA, de Oliveira HP (2019) Wearable supercapacitors based on graphene nanoplatelets/carbon nanotubes/polypyrrole composites on cotton yarns electrodes. SN Appl Sci 1:4. https://doi.org/10.1007/s42452-019-0343-5
12. Love CA, Cook RB, Harvey TJ, Dearnley PA, Wood RJK (2013) Diamond like carbon coatings for potential application in biological implants—a review. Tribol Int 63:141–150. https://doi.org/10.1016/j.triboint.2012.09.006
13. Xu J, Duan Z, Qiao L, Chai L, Chen Z, Guo D, Wang P, Liu W (2019) Nonuniform transitions of heavy-ion irradiated a-C:H films: structure and antiwear property degradation analysis. Carbon 146:200–209. https://doi.org/10.1016/j.carbon.2019.02.009
14. Liu Z, Zheng S, Lu Z, Pu J, Zhang G (2018) Adhesive transfer at copper/diamond interface and adhesion reduction mechanism with fluorine passivation: a first-principles study. Carbon 127:548–556. https://doi.org/10.1016/j.carbon.2017.11.027
15. Jurewicz AJG, Burnett DS, Rieck KD, Hervig R, Friedmann TA, Williams P, Daghlian CP, Wiens R (2017) Understanding heterogeneity in genesis diamond-like carbon film using SIMS analysis of implants. J Mater Sci 52(19):11282–11305. https://doi.org/10.1007/s10853-017-1267-3
16. Hidalgo-Manrique P, Lei X, Xu R, Zhou M, Kinloch IA, Young RJ (2019) Copper/graphene composites: a review. J Mater Sci 54(19):12236–12289. https://doi.org/10.1007/s10853-019-03703-5
17. Cui L, Lu Z, Wang L (2013) Toward low friction in high vacuum for hydrogenated diamond like carbon by tailoring sliding interface. ACS Appl Mater Interfaces 5(13):5889–5893. https://doi.org/10.1021/am401192u
18. Casiraghi C, Robertson J, Ferrari AC (2007) Diamond-like carbon for data and beer storage. Mater Today 10(1–2):44–53. https://doi.org/10.1016/s1369-7021(06)71791-6
19. Wei X, Zhang M, Shang L, Wang Y, Lu Z, Zhang G (2019) Enhancement in the corrosive and tribological properties of the inner wall of 6063Al and CI pipes by thick multilayer Si-DLC coatings. Mater Res Express 6(8):085634. https://doi.org/10.1088/2053-1591/ab28f1
20. Erdemir A (2004) Genesis of superlow friction and wear in diamondlike carbon films. Tribol Int 37(11–12):1005–1012. https://doi.org/10.1016/j.triboint.2004.07.018
21. Shi J, Wang Y, Gong Z, Zhang B, Wang C, Zhang J (2017) Nanocrystalline graphite formed at fullerene-like carbon film frictional interface. Adv Mater Interfaces 4(8):1601113. https://doi.org/10.1002/admi.201601113
22. Rao J, Cruz R, Lawson KJ, Nicholls JR (2005) Sputtered DLC-TiB2 multilayer films for tribological applications. Diam Relat Mater 14(11–12):1805–1809. https://doi.org/10.1016/j.diamond.2005.06.015
23. Cui L, Zhou H, Zhang K, Lu Z, Wang X (2018) Bias voltage dependence of superlubricity lifetime of hydrogenated amorphous carbon films in high vacuum. Tribol Int 117:107–111. https://doi.org/10.1016/j.triboint.2017.08.020
24. Kuwahara T, Romero PA, Makowski S, Weihnacht V, Moras G, Moseler M (2019) Mechano-chemical decomposition of

organic friction modifiers with multiple reactive centres induces superlubricity of ta-C. Nat Commun 10(1):151. https://doi.org/10.1038/s41467-018-08042-8
25. Voevodin AA, Phelps AW, Zabinski JS, Donley MS (1996) Friction induced phase transformation of pulsed laser deposited diamond-like carbon. Diam Relat Mater 5(11):1264–1269. https://doi.org/10.1016/0925-9635(96)00538-9
26. Bai S, Onodera T, Nagumo R, Miura R, Suzuki A, Tsuboi H, Hatakeyama N, Takaba H, Kubo M, Miyamoto A (2012) Friction reduction mechanism of hydrogen- and fluorine-terminated diamond-like carbon films investigated by molecular dynamics and quantum chemical calculation. J Phys Chem C 116(23):12559–12565. https://doi.org/10.1021/jp300937n
27. Chen X, Zhang C, Kato T, Yang XA, Wu S, Wang R, Nosaka M, Luo J (2017) Evolution of tribo-induced interfacial nanostructures governing superlubricity in a-C:H and a-C:H: Si films. Nat Commun 8(1):1675. https://doi.org/10.1038/s41467-017-01717-8
28. Kuwahara T, Moras G, Moseler M (2017) Friction regimes of water-lubricated diamond (111): role of interfacial ether groups and tribo-induced aromatic surface reconstructions. Phys Rev Lett 119(9):096101. https://doi.org/10.1103/PhysRevLett.119.096101
29. Konicek AR, Grierson DS, Gilbert PU, Sawyer WG, Sumant AV, Carpick RW (2008) Origin of ultralow friction and wear in ultrananocrystalline diamond. Phys Rev Lett 100(23):235502. https://doi.org/10.1103/PhysRevLett.100.235502
30. Pastewka L, Moser S, Gumbsch P, Moseler M (2011) Anisotropic mechanical amorphization drives wear in diamond. Nat Mater 10(1):34–38. https://doi.org/10.1038/nmat2902
31. Cui L, Lu Z, Wang L (2014) Probing the low-friction mechanism of diamond-like carbon by varying of sliding velocity and vacuum pressure. Carbon 66:259–266. https://doi.org/10.1016/j.carbon.2013.08.065
32. Berman D, Deshmukh SA, Sankaranarayanan SK, Erdemir A, Sumant AV (2015) Friction. Macroscale superlubricity enabled by graphene nanoscroll formation. Science 348(6239):1118–1122. https://doi.org/10.1126/science.1262024
33. Qi ZQ, Meletis EI (2005) Mechanical and tribological behavior of nanocomposite multilayered Cr/a-C thin films. Thin Solid Films 479(1–2):174–181. https://doi.org/10.1016/j.tsf.2004.12.009
34. Chen L, Guo P, Li X, Liu X, Zhang G, Lu Z (2019) Experimental and model studies about the lubrication of physisorbed isobutane molecules on hydrogenated diamond-like carbon films. Surf Coat Technol 357:759–767. https://doi.org/10.1016/j.surfcoat.2018.10.078
35. Shahsavari F, Ehteshamzadeh M, Naimi-Jamal MR, Irannejad A (2016) Nanoindentation and nanoscratch behaviors of DLC films growth on different thickness of Cr nanolayers. Diam Relat Mater 70:76–82. https://doi.org/10.1016/j.diamond.2016.10.003
36. Arias DF, Gómez A, Vélez JM, Souza RM, Olaya JJ (2015) A mechanical and tribological study of Cr/CrN multilayer coatings. Mater Chem Phys 160:131–140. https://doi.org/10.1016/j.matchemphys.2015.04.015
37. He D, Pu J, Lu Z, Wang L, Zhang G, Xue Q (2017) Simultaneously achieving superior mechanical and tribological properties in WC/a-C nanomultilayers via structural design and interfacial optimization. J Alloys Compd 698:420–432. https://doi.org/10.1016/j.jallcom.2016.12.173
38. He D, Li X, Pu J, Wang L, Zhang G, Lu Z, Li W, Xue Q (2018) Improving the mechanical and tribological properties of TiB2/a-C nanomultilayers by structural optimization. Ceram Int 44(3):3356–3363. https://doi.org/10.1016/j.ceramint.2017.11.125
39. Xu JH, Hattori K, Seino Y, Kojima I (2002) Microstructure and properties of CrN/$Si_3N_4$ nano-structured multilayer films. Thin Solid Films 414(2):239–245. https://doi.org/10.1016/S0040-6090(02)00483-2
40. Song G-h, Luo Z, Li F, Chen L-j, He C-l (2015) Microstructure and indentation toughness of Cr/CrN multilayer coatings by arc ion plating. Trans Nonferrous Metals Soc 25(3):811–816. https://doi.org/10.1016/s1003-6326(15)63667-6
41. Robertson J (2002) Diamond-like amorphous carbon. Mater Sci Eng R 37:129–281. https://doi.org/10.1016/S0927-796X(02)00005-0
42. Manimunda P, Al-Azizi A, Kim SH, Chromik RR (2017) Shear-induced structural changes and origin of ultralow friction of hydrogenated diamond-like carbon (DLC) in dry environment. ACS Appl Mater Interfaces 9(19):16704–16714. https://doi.org/10.1021/acsami.7b03360
43. Chen L, Wang J, Shang L, Lu Z, Wu Z, Zhang G (2019) Gas phase lubrication on diamond-like carbon film: tribochemical reactions under isobutane condition. Tribol Int 133:152–159. https://doi.org/10.1016/j.triboint.2019.01.004
44. Polaki SR, Kumar N, Madapu K, Ganesan K, Krishna NG, Srivastava SK, Abhaya S, Kamruddin M, Dash S, Tyagi AK (2016) Interpretation of friction and wear in DLC film: role of surface chemistry and test environment. J Phys D Appl Phys 49(44):445302. https://doi.org/10.1088/0022-3727/49/44/445302
45. Salinas-Rodriguez A, Rodriguez-Galicia JL (1996) Deformation behavior of low-carbon Co–Cr–Mo alloys for low-friction implant applications. J Biomed Mater Res 31(3):409–419. https://doi.org/10.1002/(SICI)1097-4636(199607)31:3%3c409:AID-JBM16%3e3.0.CO;2-D